Article

Noble Metal Nanocrystals: Plasmon Electron Transfer Photochemistry and Single-Molecule Raman Spectroscopy

Louis Brus

More About This Article

Additional resources and features associated with this article are available within the HTML version:

- Supporting Information
- Access to high resolution figures
- Links to articles and content related to this article
- Copyright permission to reproduce figures and/or text from this article

View the Full Text HTML

Noble Metal Nanocrystals: Plasmon Electron Transfer Photochemistry and Single-Molecule Raman Spectroscopy

LOUIS BRUS

Chemistry Department, Columbia University, New York, New York 10027

RECEIVED ON JUNE 23, 2008

CONSPECTUS

The excited electronic states of noble metal Au and Ag nanocrystals are very different than those of molecules. Ag and Au nanocrystal optical transitions (plasmons) in the visible can be so intense that they significantly modify the local electromagnetic field. Also, coherent elastic Rayleigh light scattering is stronger than normal electronic absorption of photons for larger nanocrystals. These two facts make Au and Ag nanocrystals ideal nanoantennas, in that they focus incident light into the local neighborhood of subwavelength size. Surface-enhanced Raman scattering (SERS), in which the Raman scattering rate of nearby molecules increases by many orders of magnitude, is a consequence of this nanoantenna effect. Metallic nanocrystals also have no band gap; this makes them extraordinarily polarizable. Their electronic transitions sense the local environment. An extreme case is the interaction of two 30 nm Ag nanocrystals separated by a 1 nm gap. Their mutual polarization completely transforms the nature of the metallic excited electronic state. Single particles have an excited state uniformly distributed throughout the interior, while the nanocrystal dimer has its excited state localized on the metal surface in the junction. This creates an electromagnetic "hot spot" in the junction, enabling the observation of single-molecule SERS. The fact that surface molecules are typically chemisorbed and exchange electrons with the metal has interesting chemical consequences. First, the enhanced Raman intensities are controlled by quantum mechanical coupling of the molecular lowest unoccupied molecular orbital (LUMO) and highest occupied molecular orbital (HOMO) with the optically excited electrons in the metal. Second, charge-transfer photochemistry can result from metal plasmon excitation. In crystalline Ag nanocrystals the photochemistry quantum yield can be high because the nanocrystal surface dominates plasmon nonradiative relaxation. Colloidal Ag nanocrystals stabilized by sodium citrate build up a photovoltage under visible excitation, caused by irreversible "hot hole" photo-oxidation of adsorbed citrate anion. This creates a driving force for photochemical transformation of round 8 nm Ag seeds into 70 nm single-crystal disk prisms under room lights, in a novel type of light-driven Ostwald ripening.
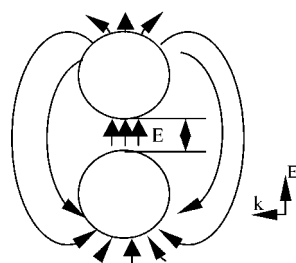
Introduction

I remember the excitement when the surface-enhanced Raman scattering (SERS) effect was discovered in the late 1970s.[1,2] The Raman scattering cross section of pyridine adsorbed on a silver electrode was enhanced by 5 or 6 orders of magnitude! It was quickly understood that this represented plasmon local electromagnetic (EM) field enhancement on a rough surface, as explained below.[3,4] Actually two different EM fields are enhanced, the incoming laser field and the outgoing Stokes-shifted field, making SERS especially dramatic. At that time, I collaborated with Abe Nitzan on the related theoretical question: whether enhanced fields would create enhanced photochemistry.[5,6] Certainly enhanced fields create an enhanced optical absorption cross section. But an excited molecule near a metal surface will undergo Förster energy transfer into the metal, and this process competes with photochemistry if the molecular excited-state lifetime is long. As it turns out the energy transfer rate falls off faster than does field enhancement, so photo-

chemistry can be enhanced at some distance above the surface.

After the initial excitement, experimental progress in SERS slowed, principally due to the extreme averaging that occurs in ensemble SERS measurements. On rough surfaces and in colloids, there is a huge distribution of molecular positions and orientations with respect to the surface and also a wide range of different field enhancements due to different local metal topologies. I went on to work with semiconductor nanocrystals, where the issue was size-dependent development of band structure.[7] Here a similar terrible ensemble averaging occurs over nanocrystal sizes, shapes, and surface stiochometry. In the 1990s, Betzig and Trautman created a significant advance in spectroscopic technique: observation of luminescence from spatially resolved single molecules and nanocrystals at 23 °C on a surface, at first using fiber optic near-field methods and subsequently confocal far-field methods.[8–11] Luminescence blinking, a signature of single molecule kinetics, was discovered in CdSe nanocrystals.

In 1997, there were two unexpected reports of single-molecule SERS for dye molecules in Ag colloids.[12,13] The combined enhancement of molecular resonance Raman and SERS was perhaps 14 orders of magnitude! The SERS single-molecule Raman signal was actually at least an order of magnitude larger than a dye molecule or semiconductor nanocrystal luminescence signal in the absence of Ag. We began to explore this discovery, using the new confocal optical methods. There are two inter-related questions: where is the single molecule on the metal, and how is this molecule so strongly coupled to the excited metallic electrons. We found that the single molecule is in a junction between particles. Study of the coupling lead us to literature quantum mechanical models for photodynamics of chemisorbed molecules. We then experimentally discovered that adsorbed citrate surfactant anions, whose SERS signals are very weak compared with the dye molecule, are actually photo-oxidized by the excited metallic "holes", creating a Ag metallic photovoltage. This photovoltage idea helps to explain recent experiments on photochemical synthesis of single-crystal Ag prisms.

Field Enhancement

The simplest formula for the optical frequency polarization dipole P created in a round particle in vacuum is

$$P = 4\pi \left(\frac{\varepsilon - 1}{\varepsilon + 2} \right) a^3 E_0 \qquad (1)$$

P is the total dipole of the particle; the polarization per cubic centimeter is uniform inside the particle volume. Here E_0 is the

electric field of the incoming light wave, a is the particle radius, and ε is the complex, wavelength-dependent particle dielectric constant.[14,15] The steady-state dipole P radiates the light wave in all directions, with a scattering rate proportional to P^2. This elastic Rayleigh scattering rate scales as a^6, that is, as the number of atoms squared. This squared dependence is the signature of a coherent effect. P is steady-state coherent polarization, not normal molecular excited-state population, which typically is in thermal equilibrium with the environment. It is the same polarization that creates reflection when a laser beam passes through a piece of glass.

In metals, P becomes very large at the wavelength for which the ac dielectric constant real part is −2. For most metals, this occurs in the vacuum ultraviolet, but for Ag, this occurs near 3800 Å. The resonant wavelength shifts into the visible and near-IR for oblong and disk shapes. The magnitude of P is limited by the small imaginary part of the resonant Ag dielectric constant: $\varepsilon = -2 + 0.2i$. This small imaginary component represents relatively slow relaxation of excited electrons in bulk crystalline Ag. In nanocrystals, excited electrons decay faster: there is additional surface-induced relaxation and for larger sizes significant radiative decay. Both these effects are not included in eq 1. This huge resonant increase in the scattering cross section is termed the dipolar plasmon. There is also a resonance in the optical photon absorption cross section, which produces heat. For small 3 nm Ag particles (and for molecules), absorption dominates scattering. But for 30 nm and larger Ag nanocrystals, scattering dominates absorption because of the square dependence on the number of atoms.

When scattering dominates, the Ag nanocrystal is essentially an ideal nanoantenna. The nanocrystal principally scatters the incident light without degrading it into heat. A nearby molecule, in the near field of P, sees a light intensity far stronger than just the intensity of the incident laser. The Ag nanocrystal concentrates, or focuses, the laser field. As a consequence, Raman scattering is faster; this appears as an enhanced cross section for molecules near the particle. For a round particle, the maximum enhancement is about 10^6 just above the surface along the direction of laser polarization. For a 100 nm Ag particle, the scattering dipole corresponds to an oscillator strength approaching 10^3. If the magnitude of P corresponds to one light quantum in the oscillator, it will radiate into the far field within a few femtoseconds. This is a very different situation than a typical excited molecule, which has a radiative lifetime of perhaps a few nanoseconds.
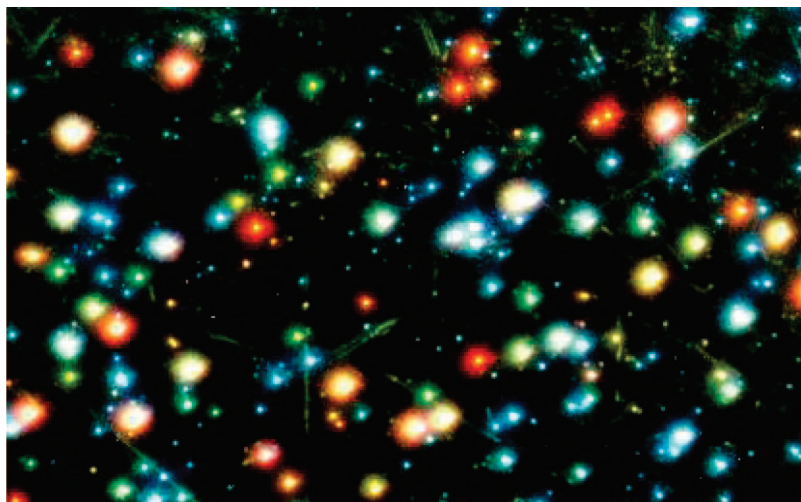
FIGURE 1. Real color photograph of dark-field scattering excited by grazing incidence white light. The sample is the spatially dispersed Ag colloid showing single-molecule SERS on an optical coverslip. The horizontal figure length is about 70 μm. Reprinted with permission in part from ref 16. Copyright 1999 American Chemical Society.

Single-Molecule Raman

Reasoning from eq 1, we thought in 1998 that a particle with intense Rayleigh (plasmon) scattering at the laser wavelength would necessarily have a huge SERS cross section; the two effects are just the far-field and near-field consequence of the same dipole *P*. Thus we measured the 90° Rayleigh scattering image and the SERS Raman image of the same field of Ag particles. The Rayleigh images were obtained in dark-field configuration with grazing incidence white light, a technique borrowed from biological imaging. The Rayleigh image in Figure 1 was striking; it showed plasmons at all different visible wavelengths.[16] The Ag colloid showing the single-molecule SERS thus has a huge range of sizes and shapes. White-light, dark-field Rayleigh scattering is quite informative and highly sensitive and has become a standard measurement.[17] Earlier, SERS particles were optically characterized mainly by the ensemble extinction spectrum in transmission.

The individual SERS Raman signals showed blinking and eventual burnout; they were clearly coming from single molecules. This has been recently confirmed by frequency domain measurement.[18] We found that our hypothesis was wrong; there was actually no correlation between the strength of the 5145 Å laser Rayleigh scattering and the strength of the SERS signal from the spatially isolated particles. When we took the AFM topology image of the same field of particles, the answer became clear: none of the "particles" that showed intense SERS were single nanocrystals. The huge SERS signals came from compact, nonfractal particle clusters, dimers or larger. Thus we concluded that the single-molecule SERS was coming from rhodamine 6G dye molecules at junctions between typically 30 nm Ag nanocrystals.[19] About the same time, this

same junction conclusion was reached by Kall and co-workers in a hemoglobin SERS study.[20] The tensor properties of the single-molecule R6G Raman scattering also confirm a uniaxial junction symmetry.[21]

There is a remarkable interaction between two close nanocrystals that creates an EM "hot spot" in the junction. In the early 1980s, this "hot spot" was found theoretically.[22,23] Assume two round nanocrystals are excited by a plane wave with polarization along the dimer axis. Exact analytical solution to Maxwell's equations shows that the SERS enhancement in the junction grows to 10^{11} and beyond as the spacing between 30 nm particles decreases to a fraction of 1 nm.[23] This is a natural situation for single-molecule Raman spectroscopy: in the limit that the two particles almost touch, there is room for only a few molecules in the junction.

While one Ag particle has its resonance at 3800 Å, the two particles together have their resonance in the green. A single oblong particle, without a junction, can also have its resonance in the green. This is the reason there is no experimental correlation between Rayleigh and Raman when the colloid has a wide range of shapes and sizes. The optimal particle radius for the touching particle dimer is 30−100 nm; beyond this, optical retardation begins to decrease enhancement in the junction. The two particle dimer is a more-or-less ideal system: retardation also tends to decrease the junction enhancement if there are additional nearby particles. Figure 2 shows a more complicated situation with three nanocrystals and three junctions, only one of which contains a R6G.

How does the metallic electronic polarization create this hot spot? We tried to understand this by direct numerical calculation of the metallic polarization inside the nanocrystals.[24]
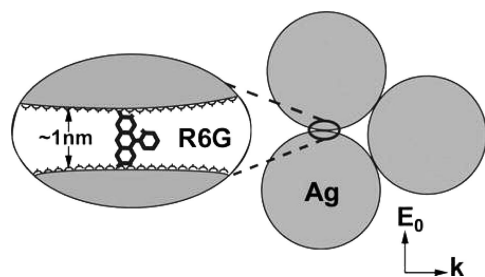
FIGURE 2. Schematic diagram of a nanocrystal trimer, drawn to scale. Only one of three junctions has a R6G molecule. The laser polarization shown is optimal for excitation of the hot spot in the junction containing R6G. All three Ag nanocrystals contribute to the plasmon far-field scattering, while only the enhanced field in the R6G junction contributes to the single-molecule Raman signal. Reprinted with permission in part from ref 24. Copyright 2003 American Chemical Society.
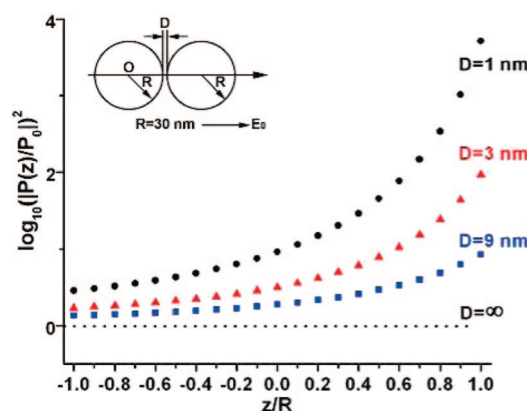

FIGURE 3. Logarithm of the normalized excited polarization density squared (per cubic centimeter) inside the metal, along the symmetry axis of the dimer. $z/R = +1$ is on the particle surface in the junction, while $z/R = -1$ is on the opposite surface away from the junction. D is the gap between the two 30 nm radius Ag nanocrystals. The volume distributed polarization density of a single nanocrystal is shown as the $D =$ infinity curve. As D becomes smaller, the polarization localizes to the metal surface in the junction. Reprinted with permission in part from ref 24. Copyright 2003 American Chemical Society.

Figure 3 shows the metallic polarization per cubic centimeter along the axis as a function of separation. Far apart, the polarization is constant; this homogeneous excitation corresponds to the dipole P excited by the laser in isolated particles. When the particles are a few angstroms apart, the metallic polarization peaks on the surface in the junction and decays toward the back surface away from the junction. Essentially, the optically excited metallic polarization ("excited state") becomes a junction surface polarization; for single particles, it is a volume polarization. Heuristically, as particles approach, the P near field of one particle excites the other particle mostly on the side facing the junction; this excitation is a quadrupole moment when expanded around the particle center. In this way, each particle excites a series of coherent higher
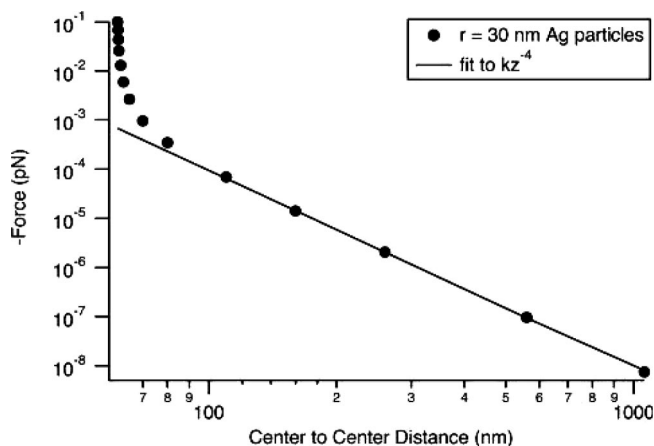

FIGURE 4. Calculated attractive optical force between two 30 nm radius Ag nanocrystals, as a function of center-to-center distance z. The incident 5145 Å light intensity is 1 kW/cm². At long range, the force is dipole−dipole, falling off as z^{-4}. At short range, the force increases above dipole−dipole by a factor of nearly 150 due to the excited metallic polarization localization on the surface in the junction. From ref 26, used with permission. Copyright 2005 National Academy of Sciences, U.S.A.

moments in the other particle.[25] Summed together, these moments form a surface polarization. This very strong mutual interaction effect is one aspect of how excited states in metal particles are so different from excited states in molecules. This is a natural consequence of the particle band gap going to zero.

Another consequence of the optical polarization localization in the junction is an enhanced optical force between the particles.[26] For laser polarization along the dimer axis, there is an attractive interaction due to the head to tail orientation of the two dipoles P. The resulting optical force, which increases linearly with the laser intensity, can be calculated by integrating the Maxwell stress tensor[27] over a particle surface. Figure 4 is a log−log force plot as a function of separation. At large separations where there is no mutual interaction, calculation shows a simple dipole−dipole force. At short separations, the force increases by 2 orders of magnitude above the extrapolated dipole−dipole force. This is an enhanced optical force from the two surface polarizations facing each other across a few angstroms in the junctions.

Exchange-Coupled SERS

How does the single R6G molecule in the junction actually interact with the excited metallic polarization? Silver and gold, which have plasmons at visible wavelengths, are noble metals without surface oxides under most conditions. A chemisorbed surface molecule directly interacts with the excited metallic polarization by electron exchange. This creates "exchange-coupled SERS", a quantum mechanical extension of

the original field enhancement SERS model. A Gauss's law argument relates the magnitude of the surface metal polarization to the enhanced *E* above the surface; the spatial regions where the surface *E* field is greatest are the regions where the surface polarization is the greatest. The enhanced field oscillates at optical frequencies. The surface polarization is microscopically composed of alternating fluxes of optically excited, coherent ballistic (undephased or unrelaxed) metallic electrons and holes, producing alternating excesses of negative and positive surface charge.

Exchange coupling controls the SERS intensities of adsorbed molecules. In the early days of SERS, it was recognized that electron exchange creates SERS cross sections that are larger than expected from simple field enhancement.[14] For example, the SERS ensemble carbon monoxide CO cross section is about 2 orders of magnitude larger than that of N_2, while the free space Raman cross sections are about the same. Also the pyridine SERS cross section on Ag is especially strong. CO and pyridine are cases where the chemisorbed molecular lowest unoccupied molecular orbital (LUMO) is resonant with the ballistic electrons of the plasmon. There can be transient localization of the optically excited metal electron on the molecule. In contrast, N_2 has a huge band gap and also adsorbs weakly on Ag. In parallel with the local field enhancement model, exchange-coupled theories of SERS have been explored.[28−30] Exchange coupling includes optical charge transfer from the molecule to the metal.[31] From the first SERS discovery, Otto has systematically championed the idea of exchange-coupled SERS.[32−34] In the single-molecule rhodamine 6G experiments with the huge SERS signals using a 5145 Å laser, there is a molecular resonance Raman effect as well as a SERS effect. Electron exchange couples the neutral excited electronic state of the dye with the neutral plasmon electron−hole polarization excited state. The R6G single-molecule Raman blinking and spectral wandering have been interpreted as chemisorption dynamics.[24,35] In the junctions, there are also adsorbed sodium citrate surfactant molecules and water molecules. These molecules, transparent to the laser, have no molecular resonance Raman effect and are not seen in single-molecule SERS.

Surface Charge-Transfer Photochemistry

Adsorbed pyridine as described above shows surface photophysics. In Figure 5, an excited metallic electron can be transiently captured in the pyridine LUMO. Pyridine evolves in structure on the anion potential surface for a few femtoseconds before the electron returns into the metal and relaxes to the Fermi level. Some excitation energy can remain in pyri-
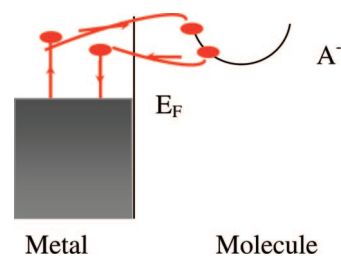

FIGURE 5. Schematic diagram of transient electron transfer from an optically excited metal nanocrystal to a chemisorbed molecule A. In the metal, the boundary between the gray and white areas is the Fermi surface. The red optically excited "hot" electron is captured by the molecular LUMO. The molecular structure briefly evolves on the anion potential surface. The electron then returns to the metal at a lower energy, and relaxes to the Fermi surface. The metal "hot hole" created by electron excitation is not shown.

dine vibrations, or the pyridine can desorb. The pyridine anion is stable, and there is no evidence that pyridine photochemistry occurs. However, in the SERS literature, there are numerous cases where changing SERS spectra indicate that some sort of photochemical process occurs as spectra are acquired.[36−39] Also, in electrochemical junctions[40,41] and on high vacuum surfaces,[42,43] reactions of "hot" excited metallic electrons with adsorbed molecules are well-known. For a good review, see ref 44.

The photochemistry quantum yield can be quite high because surface interaction dominates plasmon nonradiative dephasing in Ag nanocrystals. This can be seen in the experimental and theoretical formula for the width Γ of the dipolar plasmon in small Ag nanocrystals:[45]

$$\Gamma(a) = \Gamma_{bulk} + Av_F/a \qquad (2)$$

Here $\Gamma(a)$ is the plasmon width as a function of radius a, v_F is the Fermi velocity, and A is a constant that experimentally depends upon the surface chemical species. In bulk crystalline Ag, scattering processes causing relaxation of excited electrons and holes to the Fermi level are relatively slow; Γ_{bulk} is small, and the excited electron mean free path is long, on the order of 58 nm. It is this fact that allows P to become large in the first place. The plasmon peak experimentally broadens as particle size decreases. Equation 2, which includes the surface effect not incorporated into eq 1, was derived by Kubo, who first modeled the macroscopic EM quantity P as a quantum mechanical infinite sum of confined electron−hole pairs.[46] For a fixed size, chemisorption of specific species can strongly broaden the plasmon compared with a "clean surface". In 1993, Henglein provided a striking example:[47] Highly crystalline, round 7 nm Ag aqueous colloidal nanocrystals

show a narrow plasmon width of 0.196 eV. Iodine anion monolayer adsorption broadens the plasmon by about a factor of 3.

Thus the quantum yield for hot carrier interaction with the surface is high. The photochemistry quantum yield can also be high if irreversible chemistry occurs on the same time scale as reverse transfer of the hot carrier from the molecule to the metal.

Photovoltage from Hot "Hole" Oxidation of Adsorbed Sodium Citrate

We were fascinated by the Mirkin group discovery of a quite novel photochemical process: slow photoconversion of small colloidal 8 nm Ag nanocrystals into 70 nm disk prisms under weak illumination over a period of days.[48−54] The disk lateral dimension is controlled by matching the irradiation wavelength to the size-dependent plasmon peak of the product disk prism. Even more amazing is the sequential growth of a second, larger discrete size, without apparent formation of intermediate sizes. This occurs in an aqueous Ag colloid stabilized by adsorbed sodium citrate. Both dissolved O_2 and citrate are required for photochemistry.

Citrate is a weak reducing agent as well as an anionic surfactant. A millimolar solution of Ag^+ and excess sodium citrate at 23 °C is kinetically stable, although thermodynamically reduced metallic Ag should be made. Slow reduction does occur near 100 °C under reflux. Also, photoreduction of aqueous Ag^+ in the presence of citrate at 23 °C has been reported.[55] In 1997, Rogach et al.[56] described how UV irradiation could oxidize formic acid adsorbed on Ag nanocrystals, leading to Ag nanocrystal growth. We reasoned that plasmon excitation somehow photocatalyzed adsorbed citrate oxidation, with the extra electron quickly reducing any aqueous Ag^+ present on the outside of the double layer. To test this idea, we irradiated 8 nm Ag seeds in the presence of millimolar Ag^+ and excess citrate at 23 °C. We did see photocatalyzed growth similar to the original Mirkin experiment, with the laser wavelength controlling the lateral disk dimension.[57] After growth, if we then added a second batch of aqueous Ag^+ and also changed the laser wavelength, the particles grew further to a shape controlled by the second wavelength choice.

In a round seed, the surface flux of ballistic electron−hole pairs (i.e., surface polarization) causing photo-oxidation is highest at the two opposite poles defined by the laser polarization direction. We initially thought that the electron from citrate photo-oxidation would immediately reduce aqueous Ag^+ at the poles. If this were true then the round particle would grow oblong along the direction of the laser polarization. To test this idea, we studied growth of an adsorbed Ag
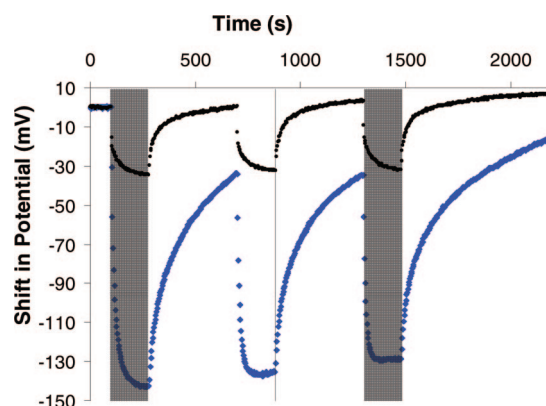

FIGURE 6. Blue trace, photoelectrochemical potential as a function of time for a silver nanocrystal working electrode in a sodium citrate aqueous solution. The shaded areas correspond to the 488 nm laser turned on. The black trace corresponds to 250 μM silver nitrate in solution in addition to citrate. A cathodic photovoltage rises to a steady state with the laser on; it decays with the laser off. The decay is faster in the presence of Ag^+. Reprinted with permission in part from ref 58. Copyright 2007 American Chemical Society.

seed on the insulating Formvar surface of a TEM grid. The dry seed was imaged in the TEM and then irradiated in a solution of citrate and Ag^+. Finally it was imaged dry again in the TEM. Our hypothesis was wrong; growth did not occur solely along the laser polarization.[58] This suggests that the extra photoelectron from citrate photo-oxidation is long-lived on the Ag seed and can reduce a Ag^+ ion anywhere on the surface. Unlike the pyridine case described above, the photo-oxidation of citrate anion is irreversible; carbon dioxide is quickly released in a Kolbe reaction.

Long-lived metallic electrons would essentially create a cathodic photovoltage. Actually, molecules do not sense voltage; they sense electric field. So in thinking about situations such as this, it is instructive to ask where does the voltage drop, where is the new electric field due to the photovoltage. This photovoltage, due to an organic anion electron becoming a Ag metallic electron, would add to the negative double layer potential created by initial citrate anion adsorption on the surface. The double layer potential would effectively increase, shifting the Ag redox potential more negative with respect the bulk solution. Electrons tunnel across the double layer to reduce aqueous Ag^+.

In Figure 6, we directly observed this photovoltage in an open-circuit electrochemical cell.[58] Citrate-stabilized Ag seeds were adsorbed on an optically transparent ITO electrode. Photovoltage rose to steady state when 5145 Å irradiation began. When the laser was turned off, the photovoltage decayed back to the rest potential. If Ag^+ were present in solution, the steady-state photovoltage was lower and the decay faster. We

studied this photovoltage as a function of Ag^+ concentration, citrate concentration, and light intensity.[59] We could fit the Ag^+ reduction rate data with the Butler–Volmer equation, which is a well-tested phenomenological activated rate theory relating redox current to applied voltage.[60] The adsorbed citrate layer slows the kinetics by many orders of magnitude compared with the reported rate on a bare Ag electrode.

Single-Crystal Prism Photochemical Synthesis at Low Light Intensities

Photovoltage helps us to understand the photochemical growth of large single-crystal Ag disk prisms from small round seeds. The mass from something like 33 small seeds combines to form one large prism. Thermodynamic formation of larger from smaller nanocrystals ("Ostwald ripening") is always favored due to the large surface energy of metals. The issue is kinetics. Neutral Ag atoms cannot transfer from smaller to larger nanocrystals because they are not soluble in water. Ag^+ ions are soluble, but if they transfer, there must be some additional process that transfers negative charge to the larger particles. For example, Ostwald ripening of bare Ag nanocrystals adsorbed on a conductive substrate in pure water is quite fast; electrons move through the substrate, and Ag^+ ions move through the water.[61] No ripening is apparent for nanocrystals adsorbed on quartz substrates.

O_2 in solution should create a low equilibrium concentration of Ag^+ due to the redox process

$$2Ag + \frac{1}{2}O_2 + H_2O \rightarrow 2Ag^+ + 2OH \qquad (3)$$
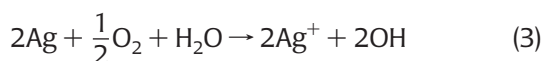
This process "etches" seeds at 23 °C, despite the presence of excess sodium citrate. Under visible irradiation, aqueous Ag^+ would preferentially reduce onto disk-shaped nanocrystals with resonant visible plasmons that develop photovoltage. The round seeds themselves have plasmons near 4000 Å on the edge of the ultraviolet. Reaction 3 would proceed to the right to keep the aqueous Ag^+ concentration constant, and the seeds would dissolve.

We quantitatively explored the photochemistry.[62] NMR measurement shows that sodium citrate is photochemically oxidized to aqueous acetone-1,3-dicarboxylate, which is unstable and simultaneously decarboxylates to form acetyl acidic acid and acetone. Yet the prism growth rate is independent of citrate concentration above 0.27×10^{-4} M, apparently because the citrate monolayer on Ag nanocrystals is complete at and above this concentration. The kinetics are autocatalytic and first-order in seed concentration, as expected if aqueous Ag^+ is independent of seed concentration. At very

low light intensity, the kinetics are linear. The rate becomes sublinear in light intensity at a quite low value, ca. 50 mW/cm^2. This may represent a switch in mechanism to Ag^+ diffusion-limited growth from Ag^+ photoreduction-limited growth. If so, then the thermodynamic Ag^+ concentration is about 10^{-9} M. The reason that two discrete sizes can be grown, as observed by Mirkin, seems to be that disk prisms of one size have two separate, distinct plasmon peaks: an intense in-plane dipole transition at longer wavelengths and a weaker quadrupole transition at shorter wavelength. Under monochromatic visible irradiation, two discrete sizes can be in resonance and develop higher photovoltage: a larger prism in resonance on its quadrupole transition and a smaller prism in resonance on its in-plane dipole transition.

Final Thoughts

In general, the theory of excited electronic states with strong correlations, such as in Ag nanocrystals, is intrinsically difficult. Our understanding of exchange-coupled SERS and of surface photochemistry remains primitive. We do not have predictive understanding. This lack of understanding encourages us to pursue basic research in this area. We do understand that the potential for surface photochemistry is high. Also, there well may be some use for hot metallic electrons in the solar energy field. There is a report of a photovoltaic cell based upon optically excited ballistic electron transfer from Au into titanium dioxide.[63]

BIOGRAPHICAL INFORMATION

Lou Brus studied chemical physics at Rice (B.A.) and at Columbia (Ph.D.), where he was a student of Rich Bersohn. He served in the U.S. Navy as Scientific Staff Officer at Naval Research Laboratory during the Vietnam War. He then spent 23 years in the chemistry and materials research area of Bell Laboratories, Murray Hill. In 1996, he returned to the chemistry department at Columbia as Professor. He has won the APS Irving Langmuir Prize, the OSA R. W. Wood Prize, and the ACS Chemistry of Materials Prize. In 1998, he was Chairman of the Board of Trustees for the Gordon Conferences.

REFERENCES

1 Jeanmaire, D.; Van Duyne, R. Surface Spectroelectrochemistry Part I: Heterocyclic Aromatic and Aliphatic Amines Adsorbed on the Anodized Silver Surface. *J. Electroanal. Chem.* **1977**, *84*, 1–20.

2 Albrecht, M.; Creighton, J. Anomalously Intense Raman Spectra of Pyridine at a Silver Electrode. *J. Am. Chem. Soc.* **1977**, *99*, 5215–5217.

3 Moskovits, M. Surface Roughness and the Enhanced Intensity of Raman Scattering by Molecules Adsorbed on Metals. *J. Chem. Phys.* **1978**, *69*, 4159–4167.

4 Creighton, J. A.; Blatchford, C. G.; Albrecht, M. G. Plasma Resonance Enhancement of Raman Scattering by Pyridine Adsorbed on Silver and Gold Sol Particles of Size Comparable to the Excitation Wavelength. *J. Chem. Soc., Faraday Trans. II* **1979**, *75*, 790–794.

5 Nitzan, A.; Brus, L. E. Can Photochemistry be Enhanced on Rough Surfaces. *J. Chem. Phys.* **1981**, *74*, 5321–5322.

6 Nitzan, A.; Brus, L. E. Theoretical Model for Enhanced Photochemistry on Rough Surfaces. *J. Chem. Phys.* **1981**, *75*, 2205–2211.

7 Rossetti, R.; Nakahara, S.; Brus, L. E. Quantum Size Effects in the Redox Potentials, Resonance Raman Spectra, and Electronic Spectra of CdS Crystallites in Aqueous Solutions. *J. Chem. Phys.* **1983**, *79*, 1086–1089.

8 Betzig, E.; Chichester, R. Near-Field Luminescence Detection of Isolated Single Molecules at Room Temperature on an Ambient Surface. *Science* **1993**, *262*, 1422–1425.

9 Trautman, J. K.; Mackllin, J. J.; Brus, L. E.; Betzig, E. Near-Field Spectroscopy of Single Molecules at Room Temperature. *Nature* **1994**, *369*, 40–42.

10 Macklin, J. J.; Trautman, J. K.; Harris, T. D.; Brus, L. E. Imaging and Time-Resolved Spectroscopy of Single Molecules at an Interface. *Science* **1996**, *272*, 255–257.

11 Nirmal, N.; Dabbousi, B. O.; Bawendi, M. G.; Macklin, J. J.; Trautman, J. K.; Harris, T. D.; Brus, L. E. Fluorescence Intermittency in Single Cadmium Selenide Nanocrystals. *Nature* **1996**, *383*, 802–805.

12 Nie, S. M.; Emery, S. R. Probing Single Molecules and Single Nanoparticles by Surface Enhanced Raman Scattering. *Science* **1997**, *275*, 1102–1106.

13 Kneipp, K.; Wang, Y.; Kneipp, H.; Perelman, L. T.; Itzkan, I.; Dasari, R.; Feld, M. S. Single Molecule Detection Using Surface Enhanced Raman Scattering. *Phys. Rev. Lett.* **1997**, *78*, 1667–1670.

14 For an early SERS review, see: Moskovits, M. Surface Enhanced Spectroscopy. *Rev. Mod. Phys.* **1985**, *57*, 783–826.

15 For a recent plasmon calculation review, see: Kelly, K. L.; Coronado, E.; Zhao, L. L.; Schatz, G. C. The Optical Properties of Metal Nanoparticles: The Influence of Size Shape and Dielectric Environment. *J. Phys. Chem. B* **2003**, *107*, 668–677.

16 Michaels, A.; Nirmal, M.; Brus, L. E. Surface Enhanced Raman Spectroscopy of Individual Rhodamine 6G Molecules on Large Ag Nanocrystals. *J. Am. Chem. Soc.* **1999**, *121*, 9932–9938.

17 Willets, K.; Van Duyne, R. Localized Surface Plasmon Resonance Spectroscopy and Sensing. *Annu. Rev. Phys. Chem.* **2007**, *58*, 267.

18 Dieringer, J.; Lettau, R.; Scheidt, K.; Van Duyne, R. A Frequency Domain Existence Proof of Single Molecule Surface Enhance Raman Spectroscopy. *J. Am. Chem. Soc.* **2007**, *129*, 16249–16256.

19 Michaels, A.; Jiang, J.; Brus, L. Ag Nanocrystal Junctions as the Site for Surface Enhanced Raman Scattering of Single Rhodamine 6G Molecules. *J. Phys. Chem. B* **2000**, *104*, 11965–11965.

20 Xu, H. X.; Bjerneld, E. J.; Kall, M.; Borjesson, L. Spectroscopy of Single Hemoglobin Molecules by Surface Enhanced Raman Scattering. *Phys. Rev. Lett.* **1999**, *83*, 4357–4360.

21 Bosnick, K.; Jiang, J.; Brus, L. Fluctuations and Local Symmetry in Single-Molecule Rhodamine 6G Raman Scattering in Silver Nanocrystal Aggregates. *J. Phys. Chem. B* **2002**, *106*, 8096–8100.

22 Aravind, P. K.; Nitzan, A.; Metiu, H. The Interaction Between Electromagnetic Resonances and Its Role in Spectroscopic Studies of Molecules Adsorbed on Colloidal Particles or Metal Spheres. *Surf. Sci.* **1981**, *110*, 189–195.

23 Inoue, M.; Ohtaka, K. Surface Enhanced Raman Scattering by Metal Spheres. 1 Cluster Effect. *J. Phys. Soc. Jpn.* **1983**, *52*, 3853–3859.

24 Jiang, J.; Bosnick, K.; Maillard, M.; Brus, L. Single Molecule Raman Spectroscopy at the Junctions of Large Ag Nanocrystals. *J. Phys. Chem. B* **2003**, *107*, 9964–9974.

25 Xu, M. L.; Dignam, M. Raman Scattering of High Density Dispersions II. *J. Chem. Phys.* **1993**, *99*, 2307–2317.

26 Hallock, J.,.; Redmond, P. L.; Brus, L. E. Optical Forces between Metallic Particles. *Proc. Nat. Acad. Sci. U.S.A.* **2005**, *102*, 1280–1283.

27 Iida, T.; Ishihara, H. Theoretical Study of the Optical Manipulation of Semiconductor Nanoparticles Under and Exciton Resonance Condition. *Phys. Rev. Lett.* **2003**, *90*, 057403.

28 Persson, B. N. J. On the Theory of Surface Enhanced Raman. *Chem. Phys. Lett.* **1981**, *82*, 561–564.

29 Nakai, H.; Nakatsuji, H. Electronic Mechanism of Surface Enhanced Raman Scattering. *J. Chem. Phys.* **1995**, *103*, 2286–2294.

30 Zhao, L.; Jensen, L.; Schatz, G. Surface Enhanced Raman Scattering of Pyrazine at the Junction Between Two Ag 20 Nanoclusters. *Nano Lett.* **2006**, *6*, 1229–12134.

31 Lombardi, J. R.; Birke, R. L.; Lu, T. Xu Charge Transfer Theory of Surface Enhanced Raman Spectroscopy: Hertzberg-Teller Contributions. *J. Chem. Phys.* **1986**, *84*, 4174–4180.

32 Otto, A. Raman Spectra of CN- Adsorbed on a Silver Surface. *Surf. Sci.* **1978**, *75*, L392–395.

33 Otto, A.; Mrozek, I.; Grabhorn, H.; Akemann, W. Surface Enhanced Raman Scattering. *J. Phys.: Condens. Mater.* **1992**, *4*, 1143–1153.

34 Otto, A.; Fukamata, M. Electronic Mechanisms of SERS. *Top. Appl. Phys.* **2006**, *103*, 147–152.

35 Weiss, A.; Haran, G. Time Dependent Surface Enhanced Raman Scattering as a Probe of Surface Dynamics. *J. Phys. Chem. B* **2001**, *105*, 12348–12353.

36 Suh, J. S.; Jang, N. H.; Jeong, D. H.; Moskovits, M. Adsorbate Photochemistry on a Colloid Surface: Phthalazine on Silver. *J. Phys. Chem.* **1996**, *100*, 805–810.

37 Jang, N. H.; Suh, J. S.; Moskovits, M. Effect of Surface Geometry on the Photochemical Reaction of 1,10-Phenanthroline Adsorbed on Silver Colloid Surfaces. *J. Phys. Chem. B* **1997**, *101*, 8279–8285.

38 Jeong, D. H.; Suh, J. S.; Moskovits, M. Enhanced Photochemistry of 2-Aminopyridine Adsorbed on Silver Colloid Surfaces. *J. Raman Spectrosc.* **2001**, *32*, 1026–1031.

39 Andersen, P. C.; Jacobson, M. L.; Rowlen, K. L. Flashy Silver Nanoparticles. *J. Phys. Chem. B* **2004**, *108*, 2148–2153.

40 Diesing, D.; Kritzler, G.; Otto, A. Surface Reactions of Hot Electrons at Metal Liquid Interfaces. *Top. Appl. Phys.* **2003**, *85*, 367–427.

41 Funkinov, A.; Sigalaev, S.; Kazarinov, V. Surface Enhanced Raman Scattering and Local Photoemission Currents on the Freshly Prepared Surface of a Silver Electrode. *J. Electroanal. Chem.* **1987**, *228*, 197–218.

42 Vondrak, T.; Burke, D.; Meech, S. Numerical Modeling of the Excitation Energy Dependence of Adsorbate Photochemistry on Metal Surfaces. *Chem. Phys. Lett.* **2001**, *347*, 1–7.

43 Pursell, D.; Dai, H. L. Photochemistry of Vinyl Chloride Physisorbed on Ag (111) Through Molecular Anion Formation by Substrate Electron Attachment. *J. Phys. Chem. B* **2006**, *110*, 10374–10379.

44 Lindstrom, C. D.; Zhu, X.-Y. Photoinduced Electron Transfer at Molecule-Metal Interfaces. *Chem. Rev.* **2006**, *106*, 4281–4300.

45 Kreibig, U.; Genzel, L. Optical Absorption of Small Metallic Particles. *Surf. Sci.* **1985**, *156*, 678–700.

46 Kawabata, A.; Kubo, R. Electronic Properties of Free Metallic Particles II Plasma Resonance Effect. *J. Phys. Soc. Jpn.* **1966**, *21*, 1765–1769.

47 Gutierrez, M.; Henglein, A. Formation of Colloidal Silver by "Push-Pull" Reduction of Silver (1+). *J. Phys. Chem.* **1993**, *97*, 11368–11370.

48 Jin, R. C.; Cao, Y. W.; Mirkin, C. A.; Kelly, K. L.; Schatz, G. C.; Zheng, J. G. Photoinduced Conversion of Silver Nanospheres into Nanoprisms. *Science* **2001**, *294*, 1901–1903.

49 Jin, R. C.; Cao, Y. C.; Hao, E. C.; Metraux, G. S.; Schatz, G. C.; Mirkin, C. A. Controlling Anisotropic Nanoparticle Growth through Plasmon Excitation. *Nature* **2003**, *425*, 487–490.

50 Callegari, A.; Tonti, D.; Chergui, M. Photochemically Grown Silver Nanoparticles of Wavelength Controlled Size and Shape. *Nano Lett.* **2003**, *3*, 1565–1568.

51 Bastys, V.; Pastoriza-Santos, I.; Rodriguez-Gonzalez, B.; Vaisnoras, R.; Liz-Marzan, L. M. Formation of Silver Nanoprisms with Surface Plasmons at Communication Wavelengths. *Adv. Funct. Mater.* **2006**, *16*, 766–773.

52 Jia, H. X.; W. An, J.; Li, D.; Zhao, B. A Simple Method to Synthesize Triangular Silver Nanoparticles by Light Irradiation. *Spectrochim. Acta, Part A* **2006**, *64*, 956–960.

53 Zheng, X.; Xu, W.; Corredor, C.; Xu, S.; An, J.; Zhao, B.; Lombardi, J. R. Laser Induced Growth of Monodisperse Silver Nanoparticles with Tunable Surface Plasmon Resonance Properties and a Wavelength Self Limiting Effect. *J. Phys. Chem. C* **2007**, *111*, 14962–14967.

54 Xue, C.; Mirkin, C. A. pH Switchable Silver Nanoprism Growth Pathway. *Angew. Chem., Int. Ed.* **2007**, *46*, 2036–2038.

55 Ahren, A.; Garrell, R. In Situ Photoreduction of Silver Nitrate as a Substrate for Surface Enhanced Raman Spectroscopy. *Anal. Chem.* **1987**, *59*, 2813–2816.

56 Rogach, A. L.; Shevchenko, G. P.; Afanaseva, Z. M.; Sviridov, V. V. Changes in the Morphology and Optical Absorption of Colloidal Silver Reduced with Formic Acid in the Polymer Matrix under UV Irradiation. *J. Phys. Chem. B* **1997**, *101*, 8129–8132.

57 Maillard, M.; Huang, P.; Brus, L. Silver Nanodisk Growth by Surface Plasmon Enhanced Photoreduction of Adsorbed [Ag^+]. *Nano Lett.* **2003**, *3*, 1611–1615.

58 Redmond, P.; Wu, X.; Brus, L. Photovoltage and Photocatalyzed Growth in Citrate-Stabilized Colloidal Silver Nanocrystals. *J. Phys. Chem. C* **2007**, *111*, 8942–8047.

59 Redmond, P.; Brus, L. E. "Hot Electron" Photo-Charging and Electrochemical Discharge Kinetics of Silver Nanocrystals. *J. Phys. Chem. C* **2007**, *111*, 14849–14854.

60 Bockris, J. O'M.; Reddy, A. K. N. *Modern Electrochemistry*; Plenum: New York, 1970; Chapter 8.

61 Redmond, P.; Hallock, A. J.; Brus, L. E. Electrochemical Ostwald Ripening of Colloidal Ag particles on Conductive Substrates. *Nano Lett.* **2005**, *5*, 131–135.

62 Wu, X.; Redmond, P. L.; Liu, H.; Chen, Y.; Steigerwald, M.; Brus, L. Photovoltage Mechanism for Room Light Conversion of Citrate Stabilized Silver Nanocrystal Seeds to Large Nanoprisms. *J. Am. Chem. Soc.* **2008**, *130*, 9500–9506.

63 McFarland, E.; Tang, J. A Photovoltaic Device Structure based upon internal electron emission. *Nature* **2003**, *421*, 618–621.